Journal of Magnetic Resonance **142,** 86–96 (2000)
Article ID jmre.1999.1918, available online at http://www.idealibrary.com on IDEAL®

Pure-Exchange Solid-State NMR

Eduardo R. deAzevedo,*,† Tito J. Bonagamba,*,† and Klaus Schmidt-Rohr*,[1]

*Department of Polymer Science & Engineering, University of Massachusetts, Amherst, Massachusetts 01003; and
†Instituto de Física de São Carlos, Universidade de São Paulo, São Paulo, Brazil

Received April 12, 1999; revised August 17, 1999

Three exchange nuclear magnetic resonance (NMR) techniques are presented that yield ^{13}C NMR spectra exclusively of slowly reorienting segments, suppressing the often dominant signals of immobile components. The first technique eliminates the diagonal ridge that usually dominates two-dimensional (2D) exchange NMR spectra and that makes it hard to detect the broad and low off-diagonal exchange patterns. A modulation of the 2D exchange spectrum by the sine-square of a factor which is proportional to the difference between evolution and detection frequencies is generated by fixed additional evolution and detection periods of duration τ, yielding a 2D pure-exchange (PUREX) spectrum. Smooth off-diagonal intensity is obtained by systematically incrementing τ and summing up the resulting spectra. The related second technique yields a static one-dimensional (1D) spectrum selectively of the exchanging site(s), which can thus be identified. Efficient detection of previously almost unobservable slow motions in a semicrystalline polymer is demonstrated. The third approach, a 1D pure-exchange experiment under magic-angle spinning, is an extension of the exchange-induced sideband (EIS) method. A TOSS (total suppression of sidebands) spectrum obtained after the same number of pulses and delays, with a simple swap of z periods, is subtracted from the EIS spectrum, leaving only the exchange-induced sidebands and a strong, easily detected centerband of the mobile site(s). © 2000 Academic Press

Key Words: **exchange NMR; segmental dynamics; chain motions; diagonal-ridge suppression.**

INTRODUCTION

Slow motions in polymers (*1–3*) and other solids have important effects on mechanical, processing, and transport properties of these materials (*4*). Multidimensional exchange NMR (*5*) of solids (*6*) in one-dimensional (1D) (*7–10*), two-dimensional (2D) (*11–14*), three-dimensional (3D) (*6, 15*), and reduced four-dimensional (4D) (*16*) versions has proven their excellent ability to characterize the time scale, geometry, orientational memory, and heterogeneity of motions on the 0.1 ms to 10 s time scale. However, these techniques have so far been limited to cases where the reorienting segments account for the major fraction of the NMR signal. Otherwise, the dominant intensity of the nonreorienting segments, for instance the high diagonal ridge in a 2D exchange spectrum, overwhelms the broader exchange intensity of the reorienting sites (*17*). This has made it practically impossible to use exchange NMR to analyze, for instance, the motion near the glass transition of the amorphous regions in semicrystalline polymers or to study side-group motion in detail without isotopic enrichment. For small frequency changes, e.g., due to small-amplitude motions, the overlap with the strong diagonal ridge is particularly severe and makes diagonal suppression desirable.

In this paper, we present three techniques for obtaining pure-exchange (PUREX) ^{13}C NMR spectra, i.e., with intensity arising only from sites reorienting during the mixing time in the experiment. The first technique, suitable for nonspinning samples or for fast magic-angle spinning, eliminates the diagonal ridge in the 2D exchange NMR spectrum while permitting flat excitation of the off-diagonal intensity. In solution NMR, such a suppression of the diagonal has been a long-standing issue addressed by a variety of approaches. These include diagonal-spectrum subtraction (*18*), modulation of the spectrum by a pulse-sequence-induced excitation function (*19, 20*), and digital removal of the diagonal signal in the time domain (*21*). In solid-state NMR, in a few cases the subtraction of a pure diagonal spectrum has been used, but it does not generally remove the diagonal ridge, as discussed below. The closest similarity of our approach is to that of Baur and Kessler (*19, 21*), which produces a sine modulation in NOESY spectra. However, in solid-state NMR, it is crucial to produce a purely positive modulation and to achieve a flat excitation of the off-diagonal intensity efficiently.

The second PUREX technique yields a static 1D spectrum selectively of the exchanging site(s), which can thus be identified. We demonstrate the efficient detection of slow segmental reorientations in a semicrystalline polymer that are almost unobservable in conventional 2D exchange experiments. The third approach, a 1D MAS experiment, is an extension of the exchange-induced sideband (EIS) method (*7*), in such a way that only a strong, easily detected centerband of the mobile site(s) and the exchange-induced sidebands are observed. It is shown that clean PUREX EIS spectra can be obtained even when the exchanging signal component is small.

[1] To whom correspondence should be addressed. E-mail: srohr@polysci.umass.edu.

1090-7807/00 $35.00

EXPERIMENTAL

Isotactic poly(1-butene) (iPB, $[-CH_2CHR-]_n$, with R = CH_2CH_3), a semicrystalline polymer with two backbone and two side-group carbon sites, of M_w = 570,000 was obtained from Aldrich. The as-received polymer pellets were prepared for NMR studies by melting at approximately 423 K, followed by slow cooling and storage at room temperature for several weeks to ensure complete conversion to crystal form I (iPB-I). Dimethyl sulfone (DMS; $O_2S(CH_3)_2$) was used in powder form as received from Aldrich.

All PUREX spectra were recorded on a Bruker DSX 300 NMR spectrometer at a ^{13}C frequency of 75 MHz. The static experiments were performed using a 5 mm static double-resonance variable-temperature Bruker probe head. For the PUREX EIS experiments, a 7 mm Bruker magic-angle spinning probe was used. No specific tune-up of individual pulse amplitudes or phases was necessary.

1D PUREX spectra on iPB-I were recorded with 1536 scans, using 90° pulse lengths of 3.9 and 4.0 μs for ^{13}C and ^{1}H, respectively. A proton decoupling field strength of approximately 90 kHz, cross-polarization time of 500 μs, signal–acquisition time of 6.2 ms, and additional evolution time τ of 500 μs were used. The experiments were performed using mixing times of 1, 10, 100, and 1000 ms.

2D PUREX ^{13}C NMR spectra on DMS were measured off-resonance in the t_1/ω_1 dimension, using 90° pulse lengths of 3.7 and 4.0 μs for ^{13}C and ^{1}H, respectively. A proton decoupling field strength of approximately 75 kHz, a cross-polarization time of 800 μs, and a t_2 acquisition time of 6.2 ms were used. In the t_1 dimension, 40 slices with increments of 48 μs were acquired. Four spectra, recorded with different values of τ (250, 500, 750, and 1000 μs), were coadded to obtain a flat modulation function across the whole off-diagonal spectrum. A total of 768 scans were acquired to obtain the PUREX spectrum. The unmodulated exchange spectrum was measured with 256 scans and 40 slices with an increment of 48 μs. The experiments were performed using mixing times of 50 ms.

2D PUREX experiments on iPB-I were performed using the same pulse lengths, proton decoupling field strength, and cross-polarization time as in the 1D PUREX experiments. In the t_1 dimension, 32 slices with an increment of 48 μs were acquired. Two spectra, with τ = 500 μs and τ = 1 ms, were recorded and coadded. Per t_1 point a total of 576 scans were acquired to obtain the PUREX spectrum. For reference, a regular exchange spectrum was measured with 96 scans and 128 slices with an increment of 48 μs. The experiments were performed using mixing times of 300 ms.

1D PUREX EIS experiments were performed at a spinning frequency of 1 kHz on a model system consisting of a mixture of approximately 90% iPB-I and 10% (13 mg) DMS. Proton decoupling field strengths of approximately $\gamma B_1/(2\pi)$ = 80 kHz, a cross-polarization time of 1000 μs, an acquisition time of 30 ms, and 90° pulse lengths of 4.3 μs for ^{13}C and 4 μs for ^{1}H were used. The experiments were performed for mixing times of 2 and 50 ms.

THEORETICAL BACKGROUND

In this section, the theoretical basis and experimental implementation of the three PUREX techniques are described.

2D PUREX Spectrum

The goal of this method is the suppression of the diagonal in a 2D exchange spectrum. It is achieved by modulation of the 2D spectrum by $\sin^2\{(\Omega_2 - \Omega_1)\tau/2\}$, where Ω_1 and Ω_2 are the precession frequencies of a given site before and after the mixing time. The most efficient way of generating this sine-square function is based on the trigonometric equalities

$$\sin^2\{(\Omega_2 - \Omega_1)\tau/2\}S = \tfrac{1}{2}(1 - \cos\{(\Omega_2 - \Omega_1)\tau\})S \quad [1]$$

$$\cos\{(\Omega_2 - \Omega_1)\tau\}S = \cos(\Omega_1\tau)\cos(\Omega_2\tau)S + \sin(\Omega_1\tau)\sin(\Omega_2\tau)S. \quad [2]$$

Here, S denotes the regular 2D exchange time or frequency signal. The two terms on the right-hand side of Eq. [2] are generated by two extra modulation periods of duration τ, one before, the other after t_m. The sine and cosine terms on the right-hand side of Eq. [2] are selected by suitable choices of the phase of the flip-back pulses (labeled e and g in Figs. 1a and 1b).

The first term $\frac{1}{2}S$ on the right-hand side of Eq. [1] corresponds to a regular 2D exchange spectrum. It is measured using the pulse sequence of Fig. 1b, which matches all pulses and relaxation delays used to acquire the $\cos\{(\Omega_2 - \Omega_1)\tau\}$-modulated spectrum in the pulse sequence of Fig. 1a. Note, for instance, that the sequences are equal before the dashed and after the dotted line. In between, only one τ delay has been moved. In order not to waste time and sensitivity on "sine–sine" scans without signal, only "cosine–cosine" terms are measured for the unmodulated spectrum. As a result, this signal requires only half the number of scans as the $\cos\{(\Omega_2 - \Omega_1)\tau\}$-modulated spectrum and has a $2^{1/2}$ times better signal-to-noise ratio.

2D PUREX Phase Cycling

The phase cycling used in the pulse sequence shown in Fig. 1a is summarized in Table 1. To obtain the complete phase cycling, the phase angles ψ and ϕ must assume independently the values 0°, 90°, 180°, and 270°, which results in a total of 128 scans per cycle. Elimination of T_1 artifacts is accomplished by inverting the phases of the pulses e and h as shown, for instance, in rows 1 and 2 of Table 1. Suppression of direct-polarization artifacts is performed by inverting the phase of the ^{1}H 90° pulse and the pulse f, as indicated in the first row by the symbol "±". Implementation of perfect quadrature detection (CYCLOPS) and suppression of

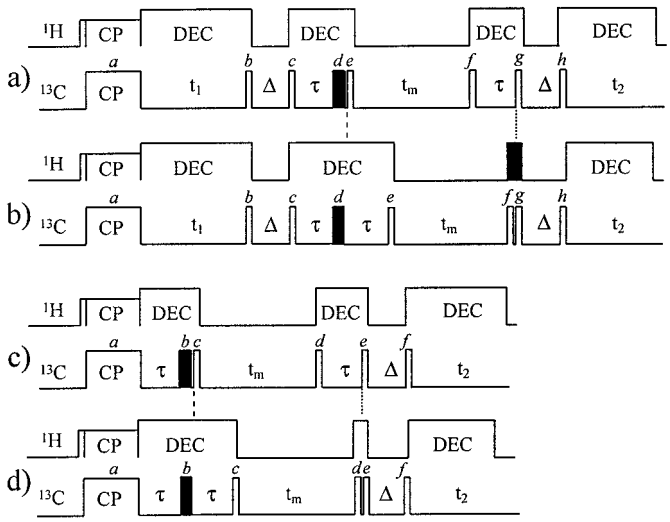

FIG. 1. Pulse sequences for static (nonspinning) PUREX experiments. (a) Two-dimensional sequence for $\cos(\Omega_2 - \Omega_1)\tau$ modulation of the 2D exchange spectrum. The 180° pulse is applied only to match the 180° pulse in (b). (b) Matching sequence without τ modulation. The spectrum obtained in (a) is acquired with twice the scans as that in (b); the difference yields the 2D PUREX spectrum. (c, d) Simplest versions of the sequence for obtaining one-dimensional static PUREX spectra, producing (c) a $\cos(\Omega_2 - \Omega_1)\tau$ modulated and (d) a matching unmodulated spectrum. To avoid artifacts resulting from long-term spectrometer drift, it is best to alternate the pulse sequences after 128 scans for (c) and 64 scans for (d), saving the two resulting spectra separately and subtracting them at the end.

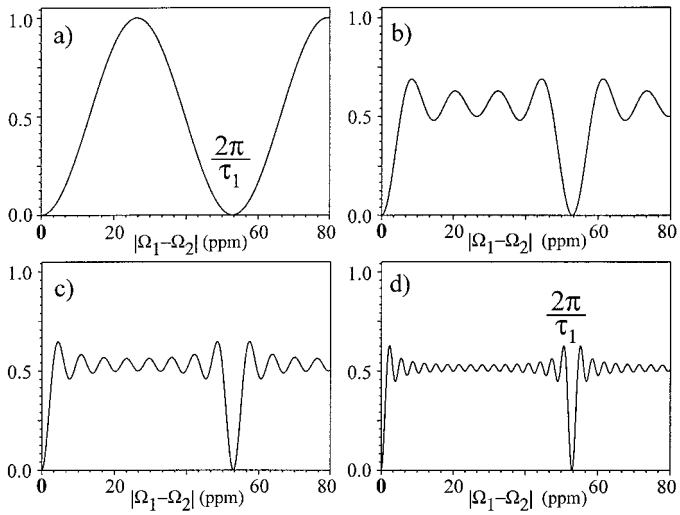

FIG. 2. Frequency-difference modulation profiles for static PUREX spectra produced by summing up signals for different numbers of τ values, systematically incremented by τ_1: (a) one τ value ($\tau_1 = 250$ μs); (b) four τ values (τ_1, $2\tau_1$, $3\tau_1$, $4\tau_1$); (c) eight τ values (τ_1, . . . , $8\tau_1$); (d) sixteen τ values (τ_1, . . . , $16\tau_1$). The modulation function in the range of $0 < |\Omega_2 - \Omega_1| < 2\pi/\tau$ approximates a constant, while it remains zero at $|\Omega_2 - \Omega_1| = 0$.

the artifacts due to imperfections in the 180° pulse (EXORCYCLE) are performed, simultaneously, by changing the pulse phases a, b, c, e, and h and the receiver phase as indicated above. The values of ψ and ϕ are set to be equal in our experiments. The phase cycling for the pulse sequence shown in Fig. 1b can be easily obtained by ignoring the rows which lead to $\sin(\Omega_1\tau)$ $\sin(\Omega_2\tau)$ components in Table 1.

Modulation Function

The desired modulation function should be flat across the whole off-diagonal spectrum, with a sharp notch along the diagonal. This can be achieved by coadding $\sin^2\{(\Omega_2 - \Omega_1)\tau/2\}$-modulated spectra for different τ values. Since all points along a straight line parallel to the diagonal have the same frequency difference $\Delta\Omega = \Omega_2 - \Omega_1$ and therefore the same modulation factor, it is sufficient to plot the modulation function along any straight line perpendicular to the diagonal. Figure 2 shows such modulation functions for sums of several $\sin^2\{(\Omega_2 - \Omega_1)\tau/2\}$ factors with a fixed τ increment. These exhibit the desired sharp notch and nearly flat top already for a small number of increments.

It is possible to modify the modulation function $W(\Delta\Omega)$, for instance to reduce the "ripple" seen in Fig. 2. This is achieved by changing the weight $f(m\tau_1)$ of the mth subspectrum. A simple Fourier relation exists between $W(\Delta\Omega)$ and $f(\tau)$:

TABLE 1
Phase Cycling for 2D PUREX[a]

	^{1}H 90°	a CP	b Store	c Read	d 180°	e Store	f Read	g Store	h Read	Receiver	Component
1	$\pm y$	$+y+\phi$	$-x+\phi$	$+x-\psi$	$-y$	$-x-\psi$	$\pm x$	$\mp x$	$+x$	$\pm y+2\psi$	$\cos(\Omega_1\tau)\cos(\Omega_2\tau)$
2	$\pm y$	$+y+\phi$	$-x+\phi$	$+x-\psi$	$-y$	$+x-\psi$	$\pm x$	$\mp x$	$-x$	$\pm y+2\psi$	$\cos(\Omega_1\tau)\cos(\Omega_2\tau)$
3	$\pm y$	$+y+\phi$	$-x+\phi$	$+x-\psi$	$-y$	$-y-\psi$	$\pm x$	$\pm y$	$-x$	$\mp y+2\psi$	$\sin(\Omega_1\tau)\sin(\Omega_2\tau)$
4	$\pm y$	$+y+\phi$	$-x+\phi$	$+x-\psi$	$-y$	$+y-\psi$	$\pm x$	$\pm y$	$+x$	$\mp y+2\psi$	$\sin(\Omega_1\tau)\sin(\Omega_2\tau)$
5	$\pm y$	$+y+\phi$	$+x+\phi$	$+x-\psi$	$-y$	$-x-\psi$	$\pm x$	$\mp x$	$+y$	$\mp x+2\psi$	$\cos(\Omega_1\tau)\cos(\Omega_2\tau)$
6	$\pm y$	$+y+\phi$	$+x+\phi$	$+x-\psi$	$-y$	$+x-\psi$	$\pm x$	$\mp x$	$-y$	$\mp x+2\psi$	$\cos(\Omega_1\tau)\cos(\Omega_2\tau)$
7	$\pm y$	$+y+\phi$	$+x+\phi$	$+x-\psi$	$-y$	$-y-\psi$	$\pm x$	$\pm y$	$-y$	$\pm x+2\psi$	$\sin(\Omega_1\tau)\sin(\Omega_2\tau)$
8	$\pm y$	$+y+\phi$	$+x+\phi$	$+x-\psi$	$-y$	$+y-\psi$	$\pm x$	$\pm y$	$+y$	$\pm x+2\psi$	$\sin(\Omega_1\tau)\sin(\Omega_2\tau)$

[a] The phase angles ϕ and ψ are incremented in 90° steps. For the sequence in Fig. 1b, only the cosine–cosine terms (rows 1, 2, 5, and 6) are acquired.

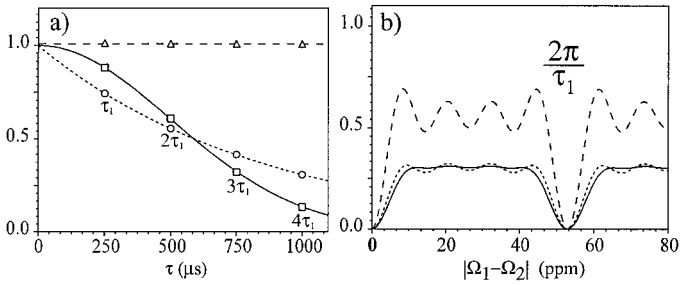

FIG. 3. (a) Gaussian (solid line) and exponential (dotted line) weighting functions used to simulate the reduction of the "ripple" in the modulation profiles compared to those resulting from the unweighted profile (dashed line). The symbols indicate the amplitudes of these functions at $\tau_1 = 250$, 500, 750, and 1000 μs. (b) Modulation profiles for static PUREX spectra produced by summing up four weighted signals with different τ values. For comparison, the modulation profiles obtained with Gaussian (solid line) or exponential (dotted line) weighting functions are shown together with the corresponding unweighted profile (dashed line).

$$W(\Delta\Omega) = \sum_{m=0}^{N} [2\sin^2(\tfrac{1}{2}\Delta\Omega m\tau_1)]\, f(m\tau_1)$$

$$\overset{(a)}{=} \sum_{m=0}^{N} [1 - \cos(\Delta\Omega m\tau_1)]\, f(m\tau_1)$$

$$\overset{(b)}{=} F - \mathrm{Re}\left(\sum_{m=0}^{N} f(m\tau_1)\exp(i\Delta\Omega m\tau_1) \right)$$

$$\overset{(c)}{=} F - \mathrm{Re}\left(\int_{-\infty}^{+\infty} f(\tau)\exp(i\Delta\Omega\tau)\, d\tau \right)$$

$$\overset{(d)}{=} F - \mathrm{Re}(\mathrm{FT}(f)). \qquad [3]$$

In step a we have used Eq. [1]. Step b is permitted because the $f(m\tau_1)$ are purely real. The constant F is the total sum of $f(m\tau_1)$. In step c the relation between a discrete and the more familiar continuous Fourier transformation has been used. It is valid if the step size τ_1 is smaller than the inverse of the width of the spectrum (i.e., fulfills the Nyquist sampling condition). Also, under these conditions, the sum F is equal to the integral over $f(\tau)$. Working purely in the framework of discrete Fourier transformation, the transition to the continuous FT could also have been skipped.

The term F in Eq. [3] is the constant corresponding to the flat regions in Fig. 2, while Re(FT(f)) is responsible for the sharp notches and the ripple. As an example, the decaying-exponential weighting function $f(m\tau_1)$ shown in Fig. 3a results in a Lorentzian notch, Fig. 3b.

Intrinsic Modulation vs Data Multiplication

It is important to note the difference between the intrinsic modulation of the signals by $\sin^2\{(\Omega_2 - \Omega_1)\tau/2\}$ and a multiplication of a regular 2D exchange pattern by $\sin^2\{(\omega_2 - \omega_1)\tau/2\}$; here, Ω_1 and Ω_2 are the actual precession frequencies, while ω_1 and ω_2 are the frequency coordinates of the 2D spectrum. With the intrinsic modulation, the 2D PUREX method suppresses not only the intensity exactly on the diagonal but also off-diagonal broadening and cutoff wiggles of the diagonal ridge. In addition to these obvious effects of relaxation and truncation, minor dead-time effects or spectrometer instabilities often cause the high diagonal ridge to produce low-level baseline distortions that have intensities similar to those of the exchange signals and are not removed by postacquisition data multiplication. PUREX with block averaging to eliminate effects of spectrometer drift reduces these artifacts by more than an order of magnitude.

In this context, it is also interesting to note that the intensity on the diagonal in the PUREX 2D spectrum does not have to be exactly zero; intrinsic or smoothing-induced line broadening can result in the wings of off-diagonal intensity extending onto the diagonal. This will occur in particular if the maximum evolution time is comparable to the maximum τ value.

With the intrinsic $\sin^2\{(\Omega_2 - \Omega_1)\tau/2\}$ modulation, the 2D PUREX spectrum has a different, and generally higher, information content than the corresponding regular 2D exchange spectrum. In the 2D PUREX spectrum, it can be distinguished whether intensity near the diagonal is the wing of a signal with exactly equal Ω_1 and Ω_2 or whether intrinsically $\Omega_1 \neq \Omega_2$.

1D PUREX Spectrum

The one-dimensional PUREX experiment derived by setting $t_1 = 0$ in the 2D PUREX pulse sequence is useful in its own right. It produces a spectrum purely of the exchanging sites, with some modulation that relates τ and the size of the frequency changes $|\Omega_2 - \Omega_1|$. Figures 1c and 1d show one-dimensional pulse sequences, suitably simplified from the 2D PUREX sequences by removal of the pulses specifically associated with the evolution time t_1. Again, the difference of the signals obtained with the two pulse sequences is recorded. To avoid artifacts due to long-term spectrometer drifts, the pulse sequences should be alternated every full phase cycle of 64 scans. The choice of τ determines whether only large frequency changes or also smaller ones are detected. The 1D PUREX spectrum can be considered as the projection of the corresponding 2D PUREX spectrum onto the ω_2 axis. This can be useful for understanding the specific modulation of the 1D PUREX spectrum.

A lower limit of the fraction f_m of sites involved in the slow dynamics can be estimated by comparing the intensities of the full 1D PUREX intensity and the corresponding full signal. The PUREX signal fraction is equal to the fraction E_∞ of the exchange intensity for very long times $t_m \gg \tau_c$ and $\tau \gg 1/\Delta\Omega$, which is related to f_m and the number M of equivalent orientation sites according to

$$E_\infty = f_m(M - 1)/M. \qquad [4]$$

For instance, the long-time PUREX signal fraction would be $E_\infty = \frac{1}{2}$ for a two-site jump ($M = 2$) of all segments ($f_m = 1$) or for half the segments ($f_m = \frac{1}{2}$) reorienting diffusively ($M \gg 1$). In terms of the modulation factors, consider that the reference signal S is compared to the PUREX signal $E_\infty(1 - \cos(\Delta\Omega\tau))S = E_\infty 2 \sin^2(\Delta\Omega\tau/2)S$, so that the PUREX signal fraction is indeed $E_\infty \times 2 \times 0.5 = E_\infty$. Note that Eq. [4] yields rigorous limits for f_m in terms of E_∞:

$$E_\infty < f_m \leq 2E_\infty. \quad [5]$$

Ultimate Resolution Limit in Exchange NMR

Based on the theory discussed so far, it would seem that with sufficient sensitivity, arbitrarily small frequency changes could be detected in PUREX spectra. This, however, is not the case. An ultimate limitation is provided by the "uncertainty relation"

$$\Delta\Omega \geq 2\pi/\tau_c; \quad [6]$$

i.e., the smallest observable frequency change $\Delta\Omega$ is comparable to the inverse of the correlation time τ_c. The origin of this limitation is most obvious in the time domain: In order to observe a frequency change of $2\pi/\tau_c$, the τ period must be of the order of τ_c. This will result in exchange during the τ period, and the premises of the simple description are violated.

PUREX EIS Spectrum

The PUREX EIS (exchange-induced sideband) technique operates on a different principle than the PUREX methods for static samples. It is based on the original EIS experiment (*7, 22*), where signal changes occur only for the sites exchanging during a mixing time inserted into a TOSS (total suppression of sidebands) pulse sequence. Otherwise, the signals are the same as in a regular TOSS spectrum. The difference between EIS and TOSS will thus yield a much simplified PUREX EIS spectrum. In addition to the exchange-induced sidebands, the PUREX EIS spectrum exhibits a strong centerband, of the same integral as the total area of the exchange-induced sidebands but of opposite sign.

In the implementation of the PUREX EIS experiment, it is paramount to make the EIS and the reference TOSS experiments as similar as possible. The pulse sequences in Figs. 4a and 4b are indeed the same except for a swap of the z periods Δ and t_m. Thus, all relaxation and pulse effects are virtually identical. At the bottom of the pulse sequences, we have indicated the necessary rotor synchronization, which ensures that the precession of the transverse magnetization is restarted at the same rotor phase at which it was interrupted by the storage pulse before t_m; in other words, t_m is equal to an integer number of rotor periods.

The most important requirement of the EIS phase cycling is the combination of both real and imaginary signal components,

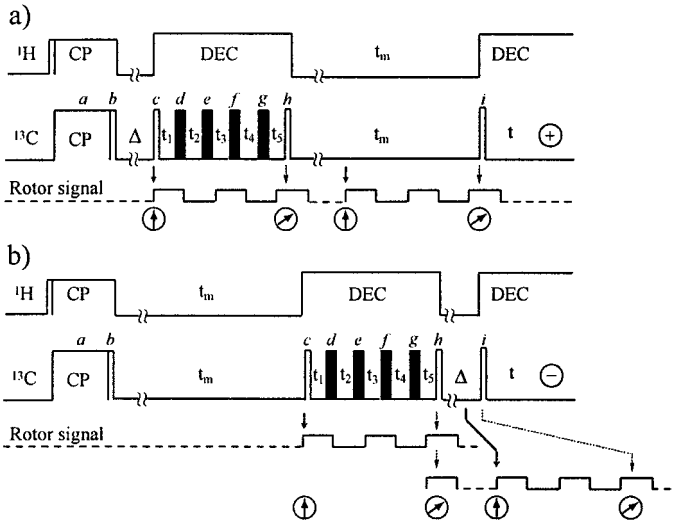

FIG. 4. Pulse sequences for a PUREX EIS experiment. At the bottom, the rotor synchronization is indicated. (a) Exchange-induced sideband (EIS) pulse sequence. (b) Matching TOSS sequence. To avoid artifacts resulting from long-term spectrometer drift, the pulse sequences are alternated after a full phase cycle of 64 scans, with inverted receiver phase for subtraction.

of which only one can be stored during the mixing time t_m, to regenerate the complex magnetization state before the storage pulse and t_m. The phase cycling used in the pulse sequence shown in Fig. 4a is summarized in Table 2. To obtain the complete phase cycling, ψ must assume the values 0°, 90°, 180°, and 270°, which results in a total of 64 scans per cycle. Elimination of T_1 and CP artifacts is accomplished, for instance, by inverting the phases of the ^{1}H 90° pulse and the receiver as indicated in rows 1 and 5. The phase shifting of the pulse h and the receiver, indicated by the symbol "$\mp$", provides the elimination of the residual transverse magnetization after the final read-out pulse, which is particularly important for acquisitions with very short mixing times. The storage during t_m of the real and imaginary parts of the magnetization, i.e., the cosine and sine components in Table 2, is performed by cycling the phase of the pulse h in the x and y directions. Additional phase cycling for compensation of experimental imperfections in the TOSS procedure (*13, 23*) is included in Table 2.

RESULTS

We have tested the three PUREX experiments on dimethyl sulfone, DMS, a crystalline organic solid which at room temperature exhibits two-site reorientations on a 10 ms time scale (*7, 22*); on isotactic poly(1-butene) form I, iPB-I, which had previously shown weak indications of exchange intensity at 258 K (*17*); and on a mixture of DMS and iPB-I at 293 K.

2D PUREX NMR

The 2D PUREX experiment is demonstrated on unlabeled DMS at ambient temperature with a mixing time $t_m = 50$ ms.

TABLE 2
Phase Cycling for PUREX EIS[a]

	^{1}H 90°	a CP	b Store	c Read	d 180°	e 180°	f 180°	g 180°	h Store	i Read	Receiver	Component
1	$+y$	$+y+\psi$	$-x+\psi$	$+x+\psi$	$-x+\psi$	$+x+\psi$	$-x+\psi$	$+y-\psi$	$\mp x-\psi$	$+x-\psi$	$\mp y-\psi$	Cosine
2	$+y$	$+y+\psi$	$-x+\psi$	$+x+\psi$	$-x+\psi$	$+x+\psi$	$-x+\psi$	$+y-\psi$	$\mp y-\psi$	$+y-\psi$	$\mp y-\psi$	Sine
3	$-y$	$+y+\psi$	$-x+\psi$	$+x+\psi$	$-x+\psi$	$+x+\psi$	$+x+\psi$	$-y-\psi$	$\mp x-\psi$	$+x-\psi$	$\pm y-\psi$	Cosine
4	$-y$	$+y+\psi$	$-x+\psi$	$+x+\psi$	$-x+\psi$	$+x+\psi$	$+x+\psi$	$-y-\psi$	$\mp y-\psi$	$+y-\psi$	$\pm y-\psi$	Sine
5	$-y$	$+y+\psi$	$-x+\psi$	$+x+\psi$	$-x+\psi$	$+x+\psi$	$-x+\psi$	$+y-\psi$	$\mp x-\psi$	$+x-\psi$	$\pm y-\psi$	Cosine
6	$-y$	$+y+\psi$	$-x+\psi$	$+x+\psi$	$-x+\psi$	$+x+\psi$	$-x+\psi$	$+y-\psi$	$\mp y-\psi$	$+y-\psi$	$\pm y-\psi$	Sine
7	$+y$	$+y+\psi$	$-x+\psi$	$+x+\psi$	$-x+\psi$	$+x+\psi$	$+x+\psi$	$-y-\psi$	$\mp x-\psi$	$+x-\psi$	$\mp y-\psi$	Cosine
8	$+y$	$+y+\psi$	$-x+\psi$	$+x+\psi$	$-x+\psi$	$+x+\psi$	$+x+\psi$	$-y-\psi$	$\mp y-\psi$	$+y-\psi$	$\mp y-\psi$	Sine

[a] The phase angle ψ is incremented in 90° steps.

DMS produces a well-defined elliptical exchange pattern, corresponding to reorientations of the CH_3 axes by 108°, which have been characterized by ^{2}H and ^{13}C exchange NMR (*14, 22*). Figure 5 shows a series of 2D PUREX spectra with corresponding simulations. The periodic modulation of the exchange intensity and the suppression of the diagonal ridge are clearly observed. The experimental and simulated spectra obtained as the sums of these patterns are displayed in Figs. 6a and 6b. The nearly uniformly excited elliptical ridge pattern is clearly seen. Only the tips of the ellipses are suppressed because the τ increment was chosen slightly too long.

For reference, a regular exchange spectrum obtained with the pulse sequence of Fig. 1b is shown in Fig. 6c. The apodization (cutoff) wiggles associated with the sharp diagonal ridge as a result of the relatively short maximum t_1 evolution time are cleanly removed in the PUREX spectrum of Fig. 6a.

1D and 2D PUREX NMR of a Semicrystalline Polymer

Regular 2D exchange experiments on iPB-I at 250 K, slightly above the glass-transition temperature, showed weak indications of exchange intensity near the highest peak along the diagonal (*17*). We now characterize the motional process by PUREX experiments. Figure 7 shows a series of 1D PUREX spectra for 1, 10, 100, and 1000 ms, taken within a total measuring time of 7 h. At the top, the regular spectrum is shown for comparison. At the bottom, the isotropic shifts of the four sites are indicated. The increase of the intensity with t_m shows that motions become significant on a 10 ms time scale and that exchange is nearly complete within 100 ms. The signals of all sites increase similarly. After $t_m = 1$ s, significant reduction of the side group signals (at low ppm values) occurs due to T_1 relaxation.

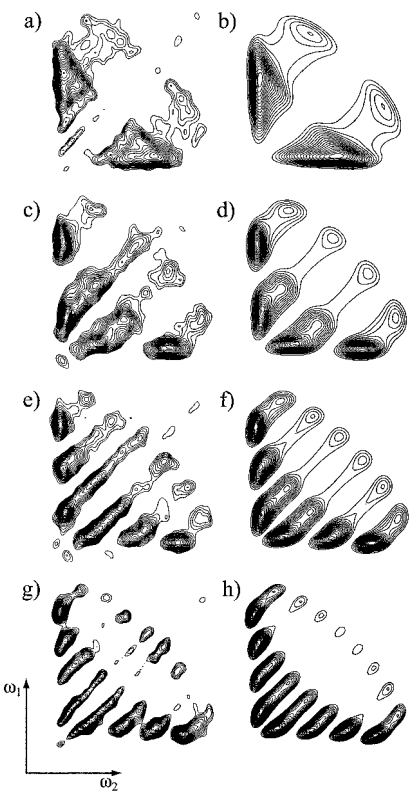

FIG. 5. 2D PUREX spectra of DMS (a) for $\tau = 250$ μs with (b) corresponding simulation, (c) for $\tau = 500$ μs with (d) simulation, (e) for $\tau = 750$ μs with (f) simulation, and (g) for $\tau = 1000$ μs with (h) simulation.

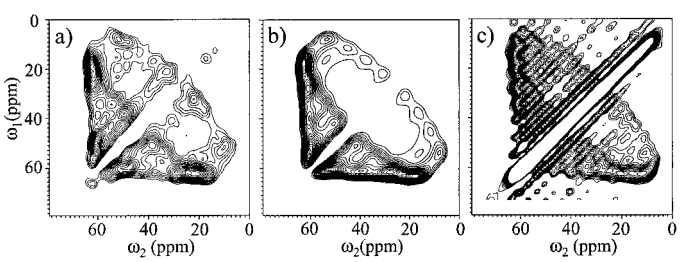

FIG. 6. (a) 2D PUREX spectrum of DMS, produced by adding the spectra for $\tau = 250$ μs to $\tau = 1$ ms shown in Fig. 5. (b) Corresponding simulation. (c) For comparison, one of the unmodulated 2D exchange spectra is shown. The strong wiggles arising from truncation of the signal in t_1 are obviously removed in the pure exchange spectrum, together with the diagonal ridge with which they are associated.

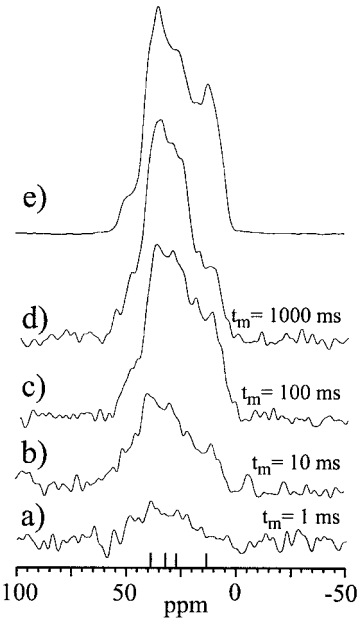

FIG. 7. Series of one-dimensional PUREX spectra of semicrystalline iPB-I at 250 K for a series of mixing times: (a) $t_m = 1$ ms; (b) $t_m = 10$ ms; (c) $t_m = 100$ ms; (d) $t_m = 1$ s; 1536 scans were averaged for each spectrum. (e) For reference, regular spectrum of iPB-I. At the bottom, the isotropic shifts of the four sites (CH_2: 38.9, 38.2; CH: 32.1; side group CH_2: 27.3, 26.5; and CH_3: 13.0 ppm) are indicated.

Figure 8 compares the 1D PUREX spectrum of iPB-I for $t_m = 1$ s with a regular spectrum obtained with the matching pulse sequence of Fig. 1d. The PUREX spectrum corresponds to approximately 25% of the reference intensity.

2D PUREX spectra with $t_m = 300$ ms and $\tau = 500$ or 1000 μs, Figs. 9a and 9b, confirm the exchange observed in the 1D spectra. All parts of the spectrum show significant exchange. The intensity along the diagonal is reduced to an insignificant fraction. Much of it actually arises from wings of off-diagonal signals, which extend to the diagonal due to strong smoothing applied to the data. The exchange intensity distribution of the sum spectrum, Fig. 9c, displays its strongest ridge in the area where the standard 2D exchange spectra, Fig. 9d and Fig. 5 of Ref. (*17*), exhibit a faint off-diagonal ridge, confirming that the same motions are observed here.

Decreasing the contour level, Fig. 9e, does not reveal the exchange pattern more clearly. Closer inspection shows that the off-diagonal ridges actually contain significant artifacts: The ridges extend beyond the square region accessible to real exchange intensity, and there are corresponding parallel negative ridges further away from the diagonal. Figure 9f shows the result of the data multiplication of the spectrum of Fig. 9d by $\{\sin^2[(\omega_1 - \omega_2)\tau_1] + \sin^2[(\omega_1 - \omega_2)\tau_2]\}$, with $\tau_1 = 500$ μs and $\tau_2 = 1$ ms. The multiplication was applied before Gaussian broadening, in order to minimize the width of the diagonal ridge. Although the diagonal ridge is indeed mostly suppressed, the artifacts are retained, making the observation of the exchange patterns still difficult.

PUREX EIS NMR

This experiment is demonstrated on a model system consisting of a mixture of ~90% iPB-I and ~10% (13 mg) DMS. The regular MAS or EIS spectrum shows only a small DMS signal, whose height is less than a quarter of that of the highest iPB-I peaks. In the EIS spectrum at a spinning speed of 1 kHz for $t_m = 50$ ms, Fig. 10a, only one very weak exchange-induced DMS sideband is observed. The PUREX EIS spectrum under the same conditions shows the exchange-induced sidebands (plotted negative) and a strong exchange-induced centerband of opposite sign for DMS, Fig. 10b. No significant iPB-I signal is detected. After a short mixing time of 2 ms, no signal is seen since, with a correlation time of ~15 ms for DMS at this temperature, little motion occurs during t_m, Fig. 10c.

DISCUSSION

2D PUREX NMR

The 2D PUREX spectrum of DMS demonstrates that this technique yields clean 2D exchange patterns without significant diagonal signal.

The sensitivity of the 2D PUREX experiment is similar to that of a regular exchange spectrum. For a single τ, the highest points in the PUREX spectrum have an intensity of 2/3 of the same points in a corresponding exchange spectrum taken in the same total measuring time. When spectra for several τ values are added up, the average intensity in the PUREX spectrum is 1/3 of that in the exchange spectrum.

Other factors compensate to a great extent for this intensity reduction. In particular, fewer t_1 points need to be acquired for the PUREX spectrum. This is possible because the PUREX spectrum exhibits a significant reduction of artifacts such as the wings of the diagonal ridge. To reduce these below the height of the exchange intensity, many more t_1 points must be mea-

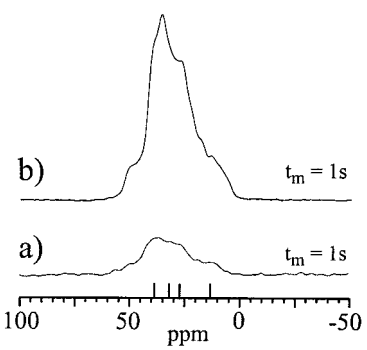

FIG. 8. Comparison of (a) a 1D PUREX spectrum ($t_m = 1$ s, $\tau = 500$ μs) of semicrystalline iPB-I, taken from Fig. 7d, with (b) a full spectrum, acquired with the pulse sequence of Fig. 1d, plotted on the same scale.

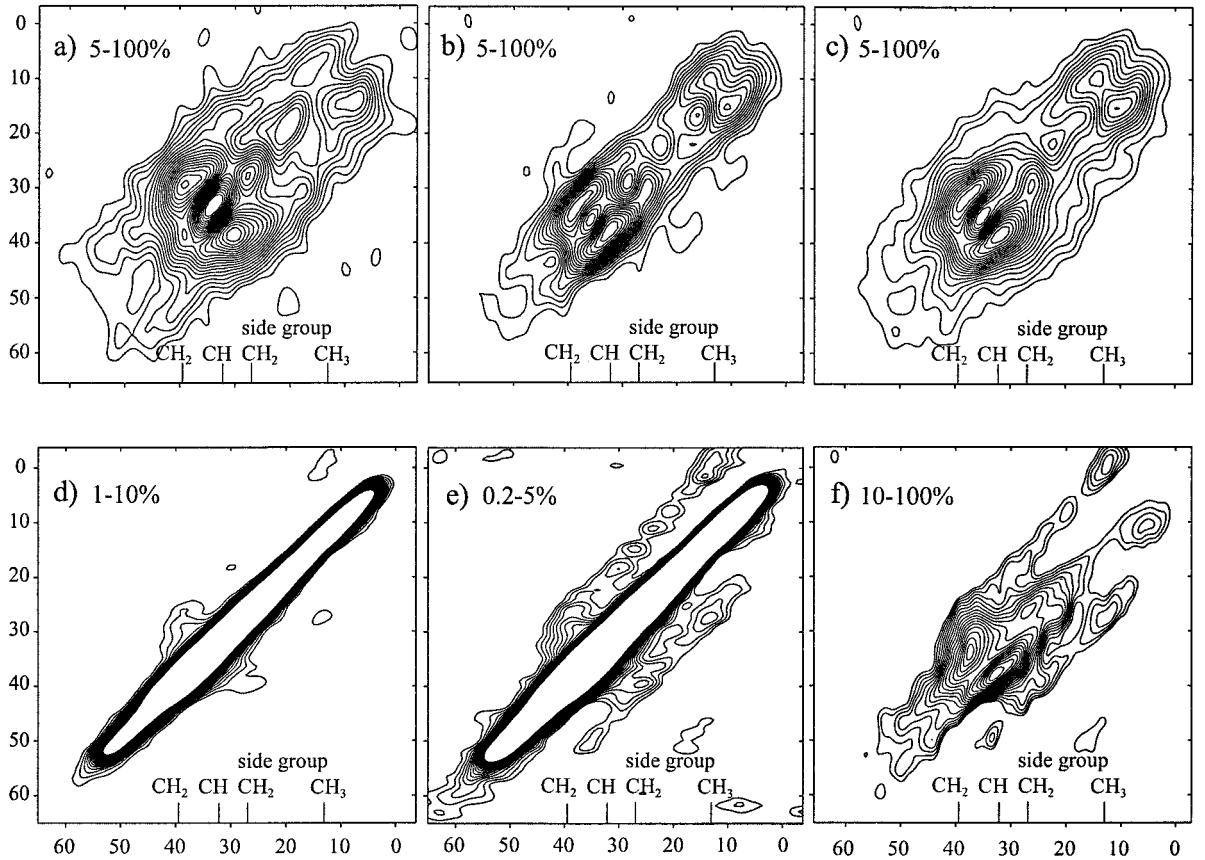

FIG. 9. Two-dimensional spectra of semicrystalline iPB-I at $T = 250$ K with $t_m = 300$ ms. At the top of each spectrum, the contour levels used are indicated as the percentage of the maximum intensity. (a) 2D PUREX spectrum with $\tau = 500$ μs. (b) 2D PUREX spectrum with $\tau = 1$ ms. For reference, the isotropic chemical shifts of the four ^{13}C sites are indicated at the bottom. (c) Sum of the spectra that are shown in (a) and (b). (d) Corresponding regular 2D exchange spectrum for comparison. This spectrum was acquired with four times more t_1 increments than the PUREX spectra in (a) and (b) to reduce cutoff wiggles of the diagonal spectrum. (e) Same as in (d) at lower contour levels. The low-level ridges that become visible contain significant artifacts that are due to the strong diagonal ridge. (f) Spectrum obtained after multiplication of the regular exchange spectrum shown in (d) and (e) by $\{\sin^2[(\omega_1 - \omega_2)\tau_1] + \sin^2[(\omega_1 - \omega_2)\tau_2]\}$, with $\tau_1 = 500$ μs and $\tau_2 = 1$ ms, and Gaussian broadening. The artifacts are not suppressed.

sured in the standard 2D exchange experiment. At these long t_1 times, the broad exchange intensity does not contribute significantly to the signal; therefore the increased number of t_1 slices only increases the measuring time and noise level. In the case of the iPB-I spectra of Fig. 9, the necessary fourfold increase of the maximum t_1 time in the standard exchange experiment leads to a nearly fourfold reduction in the off-diagonal signal-to-noise ratio, which compensates for the sensitivity reduction of the PUREX spectrum discussed above. The spectra also demonstrate clearly that the suppression of the overwhelming diagonal ridge is often much more important than a possible small reduction of the sensitivity. For applications where sensitivity is an overriding concern, the PUREX EIS experiment is recommended.

The example of iPB shows that in solid-state NMR with its broad lines, it is crucial to produce an all-positive sine-square modulation rather than the simple sine modulation previously used in solution NMR NOESY (*20*). Under the sine modulation, parts of the powder spectrum become positive and nega-

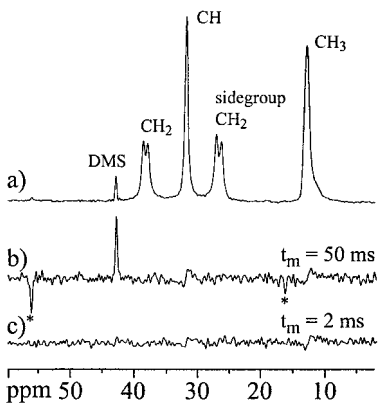

FIG. 10. PUREX EIS spectroscopy of a mixture of iPB-I and ~10% DMS at 293 K, $\omega_r/2\pi = 1$ kHz. (a) EIS spectrum with $t_m = 50$ ms. The exchange-induced sidebands of DMS are hardly visible. (b) PUREX EIS spectrum with $t_m = 50$ ms, showing the exchange centerband of DMS that matches the intensity of one strong and several weak exchange sidebands, marked by asterisks. Note the clean suppression of the strong iPB-I peaks. (c) PUREX EIS spectrum with $t_m = 2$ ms.

tive. As a result, the positive and negative signals of the various sites in iPB would cancel significantly. In addition, our scheme has a higher sensitivity, because the "1*S*" data set in Eq. [1] has the full signal.

In a way, the 2D PUREX technique presented here can be considered as a superior combination of the spectral-modulation and the diagonal-subtraction approach. In this context, it should be noted that simple subtraction of a diagonal spectrum does not generally provide a clean suppression of the diagonal ridge. If the pure-diagonal spectrum is measured with the same number of scans and subtracted unscaled, a significant negative diagonal ridge of the exchanging site will remain since its diagonal ridge was reduced by the off-diagonal intensity. If the pure-diagonal spectrum is scaled down, the diagonal may be removed for the exchanging sites, but then the nonexchanging sites would show a strong residual diagonal ridge.

2D PUREX: Intrinsic Modulation vs Data Multiplication

As discussed above, the intrinsic modulation of the PUREX signals by $\sin^2\{(\Omega_2 - \Omega_1)\tau/2\}$ is significantly different from a postacquisition multiplication of a regular 2D exchange pattern by $\sin^2\{(\omega_2 - \omega_1)\tau/2\}$. With the intrinsic modulation, the 2D PUREX method suppresses not only the intensity exactly on the diagonal but also all the spectral effects and artifacts associated with the diagonal ridge, such as off-diagonal broadening and cutoff wiggles. This is demonstrated by comparing the regular exchange spectrum of Fig. 6c with the corresponding 2D PUREX spectrum of Fig. 6a, where the cutoff wiggles are removed.

In Fig. 9, the effect is seen even more pronouncedly. Postacquisition data multiplication to suppress the diagonal ridge, Fig. 9f, leaves the artifacts unabated and appears also to retain portions of the diagonal ridge, in particular for the CH_2 signals with their larger intrinsic line broadening. Comparison of the 2D PUREX spectrum in Fig. 9c and the processed regular exchange spectrum in Fig. 9f shows clearly the greater reliability of the PUREX data.

1D PUREX NMR

The series of 1D PUREX spectra shown in Fig. 7 shows that this method is efficient at detecting partial mobility even in multisite polymers. It can identify which groups are moving and estimate the mobile fraction according to Eqs. [4] and [5]. In the case shown in Figs. 7 and 8, at least 25% of each kind of chemical group in iPB-I are found to be mobile on a 100 ms time scale. The correlation function and motional correlation time can be determined by plotting the 1D PUREX intensity as a function of the mixing time t_m; effects of T_1 relaxation during t_m are easily removed by normalization with the intensity of the reference spectrum, which is measured with the same longitudinal storage periods of total duration $t_m + 2\Delta$.

It may be interesting to note that the 1D PUREX experiment could be considered as the difference between the full signal and a pure stimulated echo (with acquisition starting at the echo maximum) (*6*, *16*, *24*, *25*). However, the standard analysis of the stimulated echo is usually incomplete in the sense that it treats only the signal corresponding to the diagonal ridge of the spectrum. The consideration of the sine-square modulated 2D pattern presented here makes the interpretation of the difference intensity much clearer. The measurement of stimulated echo decays as a function of mixing time is a similarly efficient method of determining exchange correlation times (*25*) but has so far not been used to identify specific reorienting groups. As a time-domain method, it discards the useful chemical-shift information and requires careful adjustment of the filter width for optimizing the sensitivity (*6*).

Another one-dimensional exchange experiment, selective excitation followed by a mixing time and detection, e.g., in the form of the SELDOM experiment (*8*), is much inferior to the PUREX experiments in terms of sensitivity. Selective excitation by design destroys most of the signal, whereas in the PUREX technique presented here, about half of the total signal of the mobile sites is detected.

PUREX on iPB-I

The PUREX experiments on nonspinning iPB-I show that at 250 K, significant fractions ($\geq$25%) of the sample reorient by large angles on a 100 ms time scale; see Figs. 7–9. Since the backbone sites contribute strongly to the exchange intensity, local side-group motion can be excluded as the possible origin of the exchange. Rather, overall reorientations of whole segments must be occurring. At room temperature, where the PUREX EIS spectra were taken, no slow exchange of the iPB-I signal is observed. This indicates that their motions are already faster than the millisecond time scale. Taken together, these observations indicate that the motions observed at 250 K are associated with the glass transition of the amorphous regions. We are in the process of using the PUREX techniques to confirm this hypothesis.

PUREX EIS NMR

The PUREX EIS spectra shown in Fig. 10 demonstrate that the technique works under rather difficult conditions of low absolute signal of the exchanging DMS, large nonexchanging peaks, and significant T_1 relaxation of the DMS magnetization during the mixing time. It should be noted that the PUREX EIS spectrum has good sensitivity even when compared to simple EIS: while subtracting the two spectra effectively doubles the noise in the PUREX spectrum, this factor is overcompensated by the strong intensity of the difference centerband, which is as high in magnitude as all exchange sidebands taken together (see Fig. 10).

The PUREX EIS technique works even when the sideband suppression is incomplete, which could result from pulse imperfections or partial order in the sample. If no exchange occurs, the residual sidebands appear equally in the EIS and

TOSS spectra; they will thus be subtracted out of the PUREX EIS spectrum. Only motion-induced intensity changes are observed.

^{13}C Spin-Exchange PUREX vs DOQSY NMR

The 2D exchange NMR experiment has been used not only for studying segmental dynamics but also to measure the relative orientations of segments that are close in space (*26*). The dipolar transfer of ^{13}C magnetization from one segment to another is usually referred to as ^{13}C spin exchange or ^{13}C spin diffusion. The 2D PUREX experiment can be applied unmodified to suppress the trivial and undesirable diagonal ridge arising from magnetization that remains on the given segment. However, an even superior experiment, DOQSY (*27*, *28*), exists that retains the signal of dipolar coupled segments with identical frequencies and otherwise provides essentially the same pattern as the standard 2D exchange or 2D PUREX experiment (*28*).

General Considerations

The 1D PUREX experiments combine good sensitivity with information on the nature of the exchanging sites and on the motional amplitude. They are therefore very suitable for determining motional rates efficiently. Such measurements of correlation times as a function of temperature are valuable for obtaining activation energies of the motional processes. Applications of PUREX NMR to various polymers along these lines are in progress in our laboratory. Recently, we also developed a technique for centerband-only detection of exchange, which yields PUREX MAS spectra of even higher sensitivity than the PUREX EIS method (*29*).

The 1D and 2D PUREX methods are also applicable to exchanging isotropic chemical shifts in fast magic-angle spinning or in solution NMR. Modifications of the technique for deuteron NMR are under consideration.

CONCLUSIONS

Three pure-exchange experiments have been presented which can efficiently identify and analyze dynamics of specific groups in solids of moderate to large chemical complexity. The 1D PUREX experiments, static or under MAS, combine good sensitivity with information on the nature of the exchanging sites and on the motional amplitude. They are suitable for efficient determination of motional rates and thus for obtaining activation energies. Once a suitable mixing time has thus been established, the 2D PUREX experiment can produce pure and evenly excited exchange patterns that permit the determination of the amplitude and geometry of the motion. Many applications of these methods are anticipated.

ACKNOWLEDGMENTS

Financial support by the National Science Foundation (Grant DMR-9703916) is gratefully acknowledged. E.R.dA. and T.J.B. thank the Fundação de Amparo à Pesquisa do Estado de São Paulo (FAPESP)—Brazil for fellowships. K.S.R. thanks Haskell Beckham for discussions that helped initiate this project.

REFERENCES

1. N. G. McCrum, B. E. Read, and G. Willians, "Anelastic and Dielectric Effects in Polymeric Solids," Dover, New York (1991).
2. R. H. Boyd, Relaxation processes in crystalline polymers: Molecular interpretation. A review, *Polymer* **26,** 1123–1133 (1985).
3. R. H. Boyd, Relaxation processes in crystalline polymers: Experimental behavior. A review, *Polymer* **26,** 323–347 (1985).
4. W.-G. Hu, and K. Schmidt-Rohr, Polymer ultradrawability: The crucial role of α-relaxation chain mobility in the crystallites, *Acta Polym.* **50,** 271–285 (1999).
5. R. R. Ernst, G. Bodenhausen, and A. Wokaun, "Principles of Nuclear Magnetic Resonance in One and Two Dimensions," Clarendon, New York (1992).
6. K. Schmidt-Rohr and W. Spiess, "Multidimensional Solid-State NMR and Polymers," Academic Press, London (1994).
7. Y. Yang, M. Schuster, B. Blümich, H. W. Spiess, Dynamic magic-angle spinning NMR spectroscopy: Exchange-induced sidebands, *Chem. Phys. Lett.* **139,** 239–243 (1987).
8. P. Tekely, J. Brondeau, K. Elbayed, A. Retournard, and D. Canet, Simple pulse train for selective NMR excitation in solids, *J. Magn. Reson.* **80,** 509–516 (1988).
9. V. Gerardy-Montouillout, C. Malveau, P. Tekely, Z. Olender, and Z. Luz, ODESSA, a new 1D exchange experiment for chemically equivalent nuclei in rotating solids, *J. Magn. Reson.* **123,** 7–15 (1996).
10. D. Reichert, H. Zimmermann, P. Tekely, R. Poupko, and Z. Luz, Time-reverse ODESSA. A 1D exchange experiment for rotating solids with several groups of equivalent nuclei, *J. Magn. Reson.* **125,** 245–258 (1997).
11. N. M. Szeverenyi, A. Bax, and G. E. Maciel, Proton-exchange rates in solid tropolone as measured via C13 CP/MAS NMR, *J. Am. Chem. Soc.* **105,** 2579–2582 (1983).
12. H. T. Edzes and J. P. C. Bernards, Two-dimensional exchange NMR in static powders: Interchain C-13 spin exchange in crystalline polyethylene, *J. Am. Chem. Soc.* **106,** 1515–1517 (1984).
13. A. Hagemeyer, D. Van Der Putten, and H. W. Spiess, The use of composite pulse in the TOSS experiment, *J. Magn. Reson.* **92,** 628–630 (1991).
14. C. Schmidt, B. Blümich, and H. W. Spiess, Deuteron two-dimensional exchange NMR in solids, *J. Magn. Reson.* **79,** 269–290 (1988).
15. A. Heuer, J. Leisen, S. C. Kuebler, and H. W. Spiess, Geometry and time scale of the complex rotational dynamics of amorphous polymers at the glass transition by multidimensional nuclear magnetic resonance, *J. Chem. Phys.* **105,** 7088–7096 (1996).
16. K. Schmidt-Rohr and H. W. Spiess, Nature of nonexponential loss of correlation above the glass transition investigated by multidimensional NMR, *Phys. Rev. Lett.* **66,** 3020–3023 (1991).
17. H. W. Beckham, K. Schmidt-Rohr, and H. W. Spiess, Conformation disorder and its dynamics within the crystalline phase of the form II polymorph of isotactic poly(1-butene), *in* "Multidimensional Spectroscopy of Polymers. Vibrational, NMR, and Fluorescence Tech-

niques" (M. W. Urban and T. Provder, Eds.), pp. 243–253, Am. Chem. Soc. Washington, DC (1995).

18. G. Bodenhausen and R. R. Ernst, Two-dimensional exchange difference spectroscopy. Applications to indirect observation of quadrupolar relaxation, *Mol. Phys.* **47,** 319–328 (1982).
19. M. Baur and H. Kessler, Novel suppression of the diagonal signals in the NOESY experiment, *Magn. Reson. Chem.* **35,** 877–882 (1997).
20. G. S. Harbison, J. Feigon, D. J. Ruben, and R. G. Griffin, Diagonal peak supression in 2D-NOE spectra, *J. Am. Chem. Soc.* **107,** 5567–5569 (1985).
21. G. Zhu, W. Y. Choy, G. Song, and B. C. Sanctuary, Suppression of diagonal peaks with singular value decomposition, *J. Magn. Reson.* **132,** 176–178 (1998).
22. D. Favre, D. Schaefer, S. Auerbach, and B. Chmelka, Direct measurement of intercage hopping in strongly adsorbing guest–zeolite systems, *Phys. Rev. Lett.* **81,** 5852–5855 (1998).
23. D. P. Raleigh, A. C. Kolbert, and R. G. Griffin, Effect of imperfections on TOSS spectra, *J. Magn. Reson.* **89,** 1–9 (1990).
24. C. P. Slichter, "Principles of Magnetic Resonance," Springer-Verlag, Heidelberg (1989).
25. E. Rossler, Two-dimensional exchange NMR analyzed in the time domain, *Chem. Phys. Lett.* **128,** 330–334 (1986).
26. P. Robyr, Z. Gan, and U. W. Suter, Local order between chain segments in the glassy polycarbonate of 2,2-bis(4-hydroxyphenyl)propane from ^{13}C polarization-transfer NMR, *Macromolecules* **31,** 6199–6205 (1998).
27. K. Schmidt-Rohr, A double-quantum solid-state NMR technique for determining torsion angles in polymers, *Macromolecules* **29,** 3975–3981 (1996).
28. K. Schmidt-Rohr, Complete dipolar decoupling of C-13 and its use in two-dimensional double-quantum solid-state NMR for determining polymer conformations, *J. Magn. Reson.* **131,** 209–217 (1998).
29. E. R. deAzevedo, W.-G. Hu, T. J. Bonagamba, and K. Schmidt-Rohr, Centerband-only detection of exchange: Efficient analysis of dynamics in solids by NMR, *J. Am. Chem. Soc.* **121,** 8411–8412 (1999).